Two-Nozzle Flame Synthesis of $Pt/Ba/Al_2O_3$ for NO_x Storage

Reto Strobel,[†,‡] Lutz Mädler,[†] Marco Piacentini,[‡] Marek Maciejewski,[‡] Alfons Baiker,[‡] and Sotiris E. Pratsinis*,[†]

Particle Technology Laboratory, ETH Zurich, Sonneggstrasse 3, CH-8092 Zurich, Switzerland, and Institute for Chemical and Bioengineering, ETH Zurich, Wolfgang-Pauli-Strasse 10, CH-8093 Zurich, Switzerland

Received January 9, 2006. Revised Manuscript Received March 17, 2006

A novel two-nozzle flame spray pyrolysis (FSP) process has been developed for one-step preparation of $Pt/Ba/Al_2O_3$ particles as used for NO_x storage-reduction (NSR) catalysts. The materials were characterized by transmission electron microscopy, CO chemisorption, nitrogen adsorption, X-ray diffraction, and temperature programmed decomposition and tested for their NO_x storage behavior. The use of two separate nozzles, one as aluminum and the other as a barium/platinum source, resulted in individual Al_2O_3 and monoclinic $BaCO_3$ nanoparticles, exhibiting good NO_x storage activity. In contrast, using a single-nozzle process resulted in Al_2O_3 particles with amorphous Ba species with negligible NO_x storage capacity. Increasing the internozzle distance resulted in late mixing of the two flame products and increased the amount of crystalline $BaCO_3$. At ambient conditions, as-prepared monoclinic $BaCO_3$ transformed into orthorhombic $BaCO_3$. Independent of the Ba loading, nanocrystalline $BaCO_3$ showed a low thermal stability (decomposition below 900 °C, LT-$BaCO_3$) that was distinctly different from its "bulk" behavior (decomposition above 900 °C).

Introduction

A novel, two-nozzle flame process was developed for synthesis of $Pt/Ba/Al_2O_3$ in one step allowing controlled mixing of two particle streams. Flame aerosol and in particular flame spray technologies are versatile and continuous processes for production of a variety of ceramic nanoparticles.[1−3] In contrast to spray pyrolysis, flame spray pyrolysis (FSP) is based on combustible precursor solutions, which provide the energy for the process.[3−5] A metal containing precursor solution is dispersed, ignited, and combusted. After evaporation and conversion of the metal precursor, particles are formed in the gas phase.[3,6]

Supported noble metal catalysts (i.e., Pt/Al_2O_3) consisting of Pt particles (<5 nm) finely dispersed on Al_2O_3 particles (10−40 nm) have been made by FSP.[7] Recently, FSP has also successfully been applied for the preparation of platinum supported on ceria/zirconia[8] or titania resulting in Pt clusters down to less than 2 nm for Pt loadings of 5 wt % by additional rapid quenching of the flame.[9] In general, flame-made materials are nonporous and only the external surface of the nanoparticles contributes to the high surface area[7] resulting in materials with good thermal stability.[10,11] In the case of mixed metal oxides it is rather difficult to control the distribution of two or more components in the material. As temperatures during synthesis are very high (>2000 °C) usually the thermodynamically most favored product is formed, that is, homogeneous nanoparticles (i.e., $YAlO_3$,[12] Y_2O_3/ZrO_2,[13] mullite,[14] and perovskite structures[15]) or segregated phases of different species (i.e., ZnO in SiO_2[16] and Al_2O_3/TiO_2[17]).

The $Pt/Ba/Al_2O_3$ material is of particular interest as a NO_x storage-reduction (NSR) catalyst for engines operating under lean conditions.[18,19] A decade ago, Toyota proposed the NSR concept for the NO_x abatement of lean-fuel engines.[20] According to the NSR concept, NO_x is stored under lean conditions in the form of alkali or alkaline-earth nitrates (in

* Corresponding author. Phone: +41 44 632 3180. Fax: +41 44 632 1595. E-mail: pratsinis@ptl.mavt.ethz.ch.
† Particle Technology Laboratory.
‡ Institute for Chemical and Bioengineering.

(1) Gurav, A.; Kodas, T.; Pluym, T.; Xiong, Y. *Aerosol Sci. Technol.* **1993**, *19*, 411.
(2) Pratsinis, S. E. *Prog. Energy Combust. Sci.* **1998**, *24*, 197.
(3) Mädler, L. *KONA* **2004**, *22*, 107.
(4) Okuyama, K.; Lenggoro, I. W. *Chem. Eng. Sci.* **2003**, *58*, 537.
(5) Messing, G. L.; Zhang, S. C.; Jayanthi, G. V. *J. Am. Ceram. Soc.* **1993**, *76*, 2707.
(6) Heine, M. C.; Pratsinis, S. E. *Ind. Eng. Chem. Res.* **2005**, *44*, 6222.
(7) Strobel, R.; Stark, W. J.; Mädler, L.; Pratsinis, S. E.; Baiker, A. *J. Catal.* **2003**, *213*, 296.
(8) Stark, W. J.; Grunwaldt, J. D.; Maciejewski, M.; Pratsinis, S. E.; Baiker, A. *Chem. Mater.* **2005**, *17*, 3352.
(9) Schulz, H.; Mädler, L.; Strobel, R.; Jossen, R.; Pratsinis, S. E.; Johannessen, T. *J. Mater. Res.* **2005**, *20*, 2568.
(10) Strobel, R.; Pratsinis, S. E.; Baiker, A. *J. Mater. Chem.* **2005**, *15*, 605.
(11) Stark, W. J.; Mädler, L.; Maciejewski, M.; Pratsinis, S. E.; Baiker, A. *Chem. Commun.* **2003**, 588.
(12) Marchal, J.; John, T.; Baranwal, R.; Hinklin, T.; Laine, R. M. *Chem. Mater.* **2004**, *16*, 822.
(13) Jossen, R.; Mueller, R.; Pratsinis, S. E.; Watson, M.; Akhtar, M. K. *Nanotechnology* **2005**, *16*, 609.
(14) Baranwal, R.; Villar, M. P.; Garcia, R.; Laine, R. M. *J. Am. Ceram. Soc.* **2001**, *84*, 951.
(15) Fabbrini, L.; Kryukov, A.; Cappelli, S.; Chiarello, G. L.; Rossetti, I.; Oliva, C.; Forni, L. *J. Catal.* **2005**, *232*, 247.
(16) Mädler, L.; Stark, W. J.; Pratsinis, S. E. *J. Appl. Phys.* **2002**, *92*, 6537.
(17) Kim, S.; Gislason, J. J.; Morton, R. W.; Pan, X. Q.; Sun, H. P.; Laine, R. M. *Chem. Mater.* **2004**, *16*, 2336.
(18) Kašpar, J.; Fornasiero, P.; Hickey, N. *Catal. Today* **2003**, *77*, 419.
(19) Jobson, E. *Top. Catal.* **2004**, *28*, 191.
(20) Miyoshi, N.; Matsumoto, S.; Katoh, K.; Tanaka, T.; Harada, J.; Takahashi, N.; Yokota, K.; Sugiura, M.; Kasahara, K. SAE Technical Paper 950809; Society of Automotive Engineers: Washington, DC, 1995.

10.1021/cm0600529 CCC: $33.50
Published on Web 04/22/2006

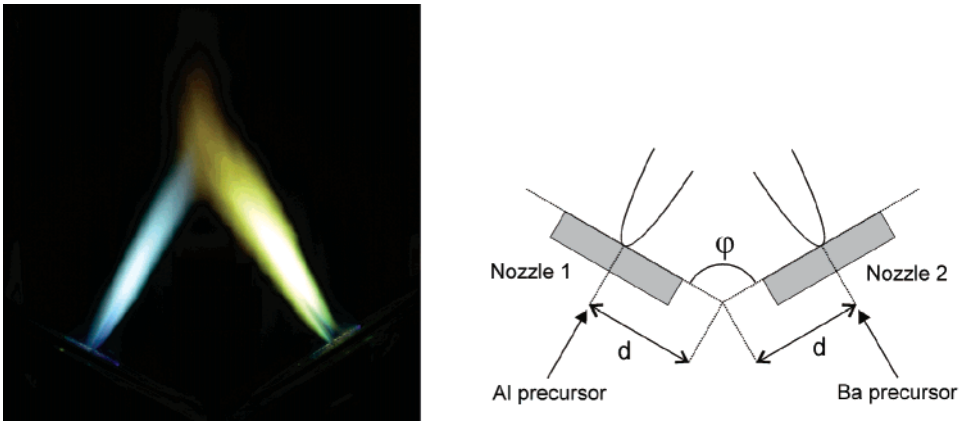

Figure 1. Schematic of the FSP setup using two separate nozzles. The image shows two flames producing Pt/Ba/Al_2O_3 (blue flame (left): Al; yellow-greenish flame (right): Pt and Ba).

particular $Ba(NO_3)_2$) and reduced over a noble metal into N_2 during fuel rich periods.[21] Generally these catalysts are prepared by wet impregnation of an alumina support from aqueous solutions of barium and platinum precursors.[21] Recently it has been shown that different Ba phases of impregnated materials strongly affect the NO_x storage capacity of Pt/Ba/Al_2O_3, and $BaCO_3$ decomposing at low temperatures (LT-$BaCO_3$) has been identified as the most active Ba species in the NO_x storage process.[22,23]

Compared to the conventional single-nozzle setup during FSP,[3] the present stereoscopic two-nozzle setup adds further flexibility for the control of important flame parameters, such as temperature and concentration fields, that affect particle formation, and affords excellent control of particle mixing at the nano-level in multicomponent systems. Here we show how a two-nozzle system can be beneficially used to control the structure of Pt/Ba/Al_2O_3 catalysts leading to enhanced NO_x storage behavior.

Experimental Section

Preparation Procedure. The setup for synthesis of Pt/Ba/Al_2O_3 consisted of two separate FSP nozzles, each able to disperse and ignite a liquid precursor solution (Figure 1). The angle between the two nozzles (φ) was fixed at 120°, and the internozzle distance between the angle tip and each nozzle center (d) was varied symmetrically between 3 and 7 cm. The individual spray nozzle was described earlier in detail.[24]

The Al precursor solution was fed at 5 mL/min through the first nozzle, and the Pt/Ba precursor solution was fed at 3 mL/min through the second nozzle by syringe pumps (Inotech). Each sprayed solution was dispersed by 5 L/min oxygen (PanGas, 99.95%) forming two fine sprays. Both sprays were surrounded and ignited by a small flame ring issuing from an annular gap (0.15 mm spacing, at a radius of 6 mm). The gas flow rates of these two individually premixed methane/oxygen supporting flames were 3.5 L/min each with a CH_4/O_2 ratio of 0.46. Product particles were collected on a glass fiber filter (Whatman GF/D, 25.7 cm in diameter) with the aid of a vacuum pump (Busch, Seco SV 1040C).

For the two-nozzle FSP two separate precursor mixtures were prepared, one containing the Al precursor and the other containing the Pt and Ba precursors. The aluminum precursor solution consisted of aluminum(III) tri-*sec*-butoxide (Alfa Aesar, 95%) dissolved in a 2:1 vol % mixture of diethylene glycol monobutyl ether (Fluka, 98%) and acetic anhydride (Riedel-de Haën, 99%). The Al concentration was kept constant at 0.5 mol/L. For the Pt/Ba precursor solution, barium(II) 2-ethylhexanoate (75% in 2-ethylhexanoic acid, Alfa Aesar, 99.8%) and platinum(II) acetylacetonate (Strem, 98%) were dissolved in ethanol (Alcosuisse, 98%). The barium and platinum concentrations were adjusted for the desired Ba and Pt content in the final product, respectively.

For comparison Pt/Ba/Al_2O_3 powder was produced also by standard, one-nozzle FSP with a precursor feed rate of 5 mL/min and oxygen dispersion gas flow rate of 5 L/min. In that precursor solution aluminum(III) tri-*sec*-butoxide, barium(II) 2-ethylhexanoate (Aldrich, 98%), and platinum(II) acetylacetonate were dissolved in toluene (Al = 0.5 mol/L).

Unless otherwise stated, the nominal Pt/Ba/Al_2O_3 weight ratio in the feed was 1:20:100. For the calculation of the nominal mass fractions of individual components, complete formation of $BaCO_3$ was assumed: A powder with the nominal ratio of 1:20:100 contains 15.4 wt % Ba and 22.9 wt % $BaCO_3$.

Materials Characterization. The specific surface area (SSA) of the as-prepared powders was determined by nitrogen adsorption at 77 K using the BET method (Micromeritics Tristar). The powder X-ray diffraction (XRD) patterns were recorded with a Bruker D8 advance diffractometer in step mode ($2\theta = 15-75°$) with a step size of 0.04° and a scan speed of 0.48°/min. The mass fraction of monoclinic $BaCO_3$ (ICSD collection code: 63257) and witherite (ICSD: 15196) was derived from the corresponding XRD patterns based on the fundamental parameter approach and the Rietveld method using the software TOPAS.[25]

Platinum dispersion was determined by CO-pulse chemisorption at 40 °C with 50 mL/min He and pulses of 0.5 mL (10% CO in He) on a Micromeritics Autochem II 2920 unit. Prior to dispersion analysis all samples were freshly reduced for 1 h at 250 °C under flowing hydrogen (20 mL/min) and then flushed by He (50 mL/min) at 260 °C for 90 min. To calculate the metal dispersion, an adsorption stoichiometry of Pt/CO = 1 was assumed.[26]

Temperature programmed decomposition (TPD) of $BaCO_3$ was measured with 35 mg of powder on a Micromeritics Autochem II 2920 in a helium flow (20 mL/min) from 50 to 1000 °C at 10 °C/min. The gas-phase composition was monitored by a mass

(21) Epling, W. S.; Campbell, L. E.; Yezerets, A.; Currier, N. W.; Parks, J. E. *Catal. Rev.* **2004**, *46*, 163.
(22) Piacentini, M.; Maciejewski, M.; Baiker, A. *Appl. Catal., B* **2005**, *59*, 187.
(23) Piacentini, M.; Maciejewski, M.; Baiker, A. *Appl. Catal., B* **2005**, *60*, 265.
(24) Mädler, L.; Stark, W. J.; Pratsinis, S. E. *J. Mater. Res.* **2002**, *17*, 1356.
(25) Cheary, R. W.; Coelho, A. A. *J. Appl. Crystallogr.* **1998**, *31*, 862.
(26) Freel, J. *J. Catal.* **1972**, *25*, 149.

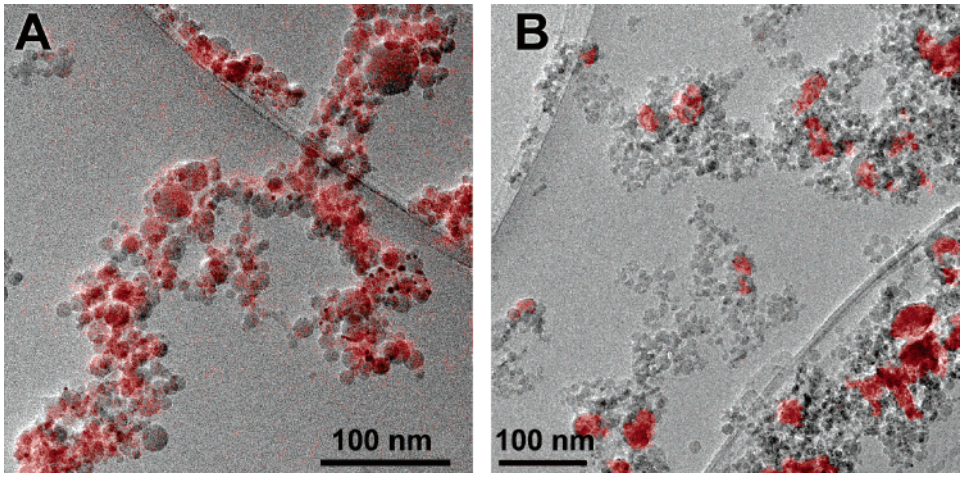

Figure 2. TEM images of flame-derived Pt/Ba/Al_2O_3 made with one nozzle (A) and two nozzles at $d = 6$ cm (B). The corresponding ESI mappings of Ba are shown as a red overlay.

spectrometer (Thermostar, Pfeiffer Vacuum). After each experiment the CO_2 signal ($m/z = 44$) was calibrated by injecting a well-defined pulse of CO_2 (0.35 mL).

For transmission electron microscopy (TEM), the material was dispersed in ethanol and deposited onto a perforated carbon foil supported on a copper grid. The investigations were performed on a Tecnai F30 microscope (FEI (Eindhoven); field emission cathode, operated at 300 kV). TEM images were recorded with a slow-scan charge-coupled device camera. An energy filter (Gatan imaging filter, GIF), which is installed below the Tecnai 30 FEG, allows recording element specific images (elemental maps) of barium (Ba-L edge at an energy loss = 781 eV) by means of the electron spectroscopic imaging (ESI) technique.[27]

NO_x storage measurements were carried out on a Netzsch STA 409 thermoanalyzer which was connected to a valve device enabling pulse thermal analysis (Pulse TA). After pretreatment of the as-prepared samples in 5 vol % O_2 in He at 500 °C for 1 h, the NO_x uptake was monitored gravimetrically during injection of NO pulses (1 mL) into 5 vol % O_2/He flow (50 mL/min) at 300 °C.[23]

Results and Discussion

Figure 1 shows a stereoscopic two-nozzle FSP unit producing Al_2O_3 particles on the left burner (blue flame) and Pt/Ba in the right one (yellow-green flame). The yellow-green color is characteristic for barium. The use of two nozzles strongly altered the structural properties of the Ba containing phase. Figure 2 shows TEM images of flame-made Pt/Ba/Al_2O_3 using one (A) and two nozzles (B), respectively. The Ba mapping as measured by ESI of the corresponding TEM pictures is shown as a red overlay. The conventional single-nozzle FSP process resulted in the distribution of Ba over all the Al_2O_3 nanoparticles (Figure 2A), whereas the material prepared with two nozzles consisted of distinct $BaCO_3$ particles (10−30 nm) that were dispersed within the Al_2O_3 particles (Figure 2B).

When the internozzle distance is increased, the mixing of the Al- and Ba-laden flames occurs further downstream at lower temperatures, and later particle formation stages reduce the high-temperature residence time of particles and the product particles size.[28] One can see that the two flame tips

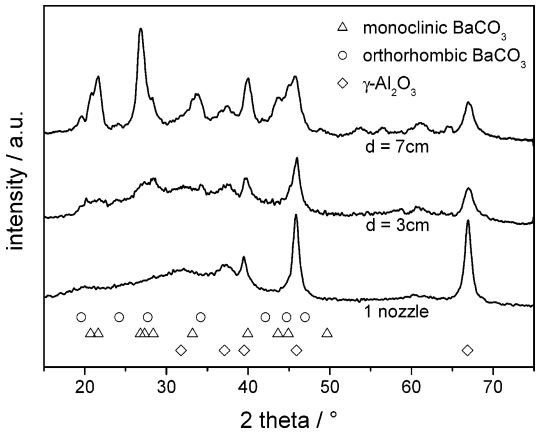

Figure 3. XRD patterns of as-prepared Pt/Ba/Al_2O_3 made with either one nozzle or two nozzles at $d = 3$ or 7 cm.

come in contact where the respective flame products start to mix (Figure 1). Considering that during FSP ceramic particle formation starts typically below the middle of the visible part of the flame,[28] both alumina and barium species formation has been well advanced by the time the two flames meet. In contrast, noble metal particles form further downstream,[9] and it is quite likely that Pt formation may take place near the point of flame mixing. This means that the Al and Ba precursors have evaporated separately in the two flames. So, Al- and Ba-containing particles have formed individually. At the point of mixing the two types of particles only agglomerate and do not sinter into a single particle as lower temperatures prevail late in the flame.[28] In contrast to this, the one-nozzle FSP process, where Al and Ba evaporate and form in the same flame, leads to particles consisting of both Al and Ba (Figure 2A) by subsequent sintering and recombination of Al and Ba particles at the high temperatures.

Powder prepared with a single FSP nozzle consisted of crystalline γ-Al_2O_3 and no crystalline Pt or Ba species could be detected (Figure 3). Considering the low Pt content (<1 wt %), this was expected for platinum.[7] Only amorphous Ba species were present. In contrast to this, crystalline $BaCO_3$ was formed with two nozzles (Figure 3): monoclinic and

(27) Grogger, W.; Hofer, F.; Warbichler, P.; Kothleitner, G. *Microsc. Microanal.* **2000**, *6*, 161.

(28) Mueller, R.; Jossen, R.; Kammler, H. K.; Pratsinis, S. E.; Akhtar, M. K. *AIChE J.* **2004**, *50*, 3085.

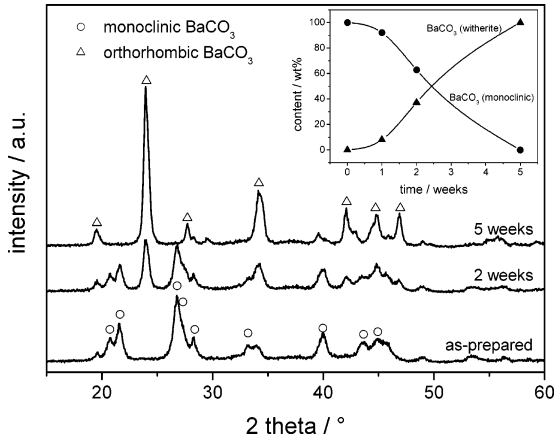

Figure 4. XRD patterns showing the transformation of monoclinic $BaCO_3$ into the thermodynamically more stable witherite as a function of time (Pt/Ba/Al_2O_3 = 1:50:100, d = 6 cm). The inset shows the corresponding amounts of monoclinic and orthorhombic $BaCO_3$ over time.

orthorhombic $BaCO_3$ (witherite) along with γ-Al_2O_3. The fraction of crystalline $BaCO_3$ increased with increasing internozzle distance (d). As $BaCO_3$ would not be stable and decompose into BaO and CO_2 at the high temperatures in the flame (<1500 °C), it can be assumed that in a first step BaO particles are formed. Later downstream at lower temperatures and when exposed to a significant amount of CO_2 from the combustion process BaO transforms into $BaCO_3$. At 1300 °C the equilibrium CO_2 partial pressure for the reaction BaO + CO_2 ↔ $BaCO_3$ would be 0.1 bar, a reasonable value for CO_2 in the flame.[29] A temperature of 1300 °C is reached at about 15 cm above the nozzle.[9,30] The formation of $BaCO_3$ instead of BaO in the flame process is not surprising as flame synthesis resulted also in the formation of $CaCO_3$,[31] which would decompose into CaO at even lower temperatures than $BaCO_3$.[29]

At ambient conditions the metastable monoclinic $BaCO_3$ of the as-prepared material was transformed into the thermodynamically stable orthorhombic form (witherite).[32,33] Figure 4 depicts this transformation for a flame-made powder (Pt/Ba/Al_2O_3 = 1:50:100, d = 6 cm). Monoclinic $BaCO_3$ was transformed completely into pure orthorhombic $BaCO_3$ (witherite) over a time period of approximately 1 month. The formation of this metastable monoclinic phase was also observed for unsupported flame-made $BaCO_3$ and can be attributed to the rapid quenching during flame synthesis.[34] In general, the steep cooling during flame synthesis often results in metastable phases or high-temperature modifications as reported, for example, for ZrO_2[35] or Y_2O_3.[36]

Figure 5 shows the $BaCO_3$ decomposition as measured by CO_2-TPD (m/z = 44) for powders made with one nozzle and two nozzles placed at different distances. The CO_2 evolution below 300 °C corresponds to CO_2 desorption from the particle surface. The peaks between 200 and 400 °C can be attributed to combustion of carbon-containing impurities with some residual oxygen as the CO_2 evolution was accompanied by water evolution (m/z = 18). The main peak occurring at about 600 °C arises from $BaCO_3$ decomposition into BaO and CO_2. This temperature is much lower than that of bulk $BaCO_3$ decomposing between 900 and 1200 °C.[22] For all two-nozzle FSP-made Ba-containing powders only the so-called LT-$BaCO_3$ (T_d < 900 °C) and no HT-$BaCO_3$ (T_d > 900 °C) was observed.[22] Particles made with one nozzle showed CO_2 evolution only from desorption of surface CO_2 species and virtually nothing from $BaCO_3$ decomposition. At increased internozzle distances more CO_2 evolved consistent with XRD observations (Figure 3).

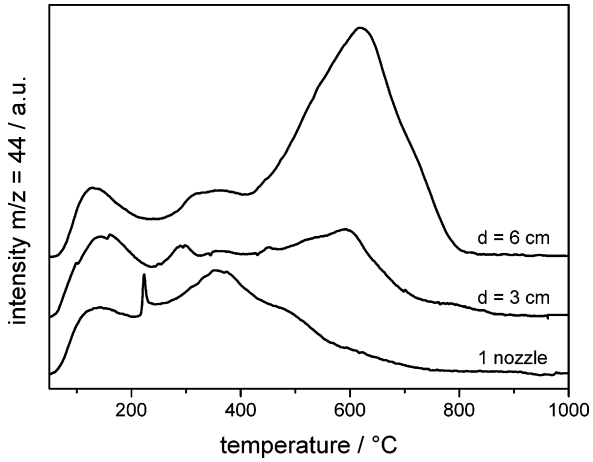

Figure 5. TPD CO_2 evolution profiles during decomposition of $BaCO_3$ for as-prepared Pt/Ba/Al_2O_3 from one or two nozzles at internozzle distances (d) of 3 and 6 cm.

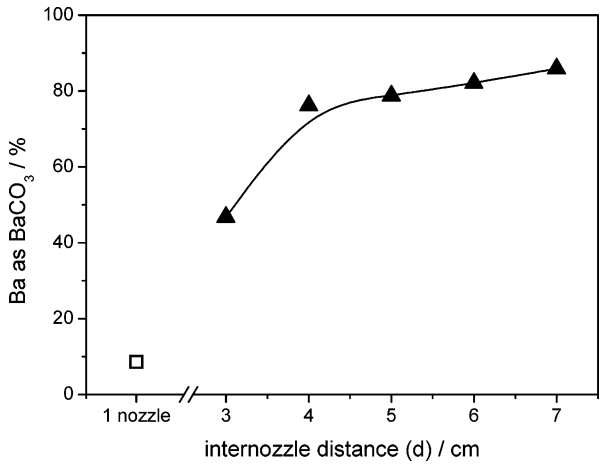

Figure 6. Relative amount of Ba in the form of $BaCO_3$ as a function of internozzle distance (d) for Pt/Ba/Al_2O_3. Increasing d resulted in later mixing of Ba with Al at lower temperatures favoring less interaction of Ba with Al that limits the formation of $BaCO_3$. For this reason Pt/Ba/Al_2O_3 prepared with one nozzle contained virtually no $BaCO_3$.

Figure 6 depicts the relative amount of Ba in the form of $BaCO_3$ for Pt/Ba/Al_2O_3 prepared with one and two nozzles. The amount of $BaCO_3$ was derived from TPD profiles (Figure 5) by integrating the amount of CO_2 evolved above 400 °C to distinguish from CO_2 desorption. Figure 6 clearly shows that more $BaCO_3$ is formed when using the two-nozzle

(29) Stern, K. H.; Weise, E. L. *Natl. Stand. Ref. Data Ser.* **1969**, *30*, 1.
(30) Mädler, L.; Kammler, H. K.; Mueller, R.; Pratsinis, S. E. *J. Aerosol Sci.* **2002**, *33*, 369.
(31) Huber, M.; Stark, W. J.; Loher, S.; Maciejewski, M.; Krumeich, F.; Baiker, A. *Chem. Commun.* **2005**, 648.
(32) Lietti, L.; Forzatti, P.; Nova, I.; Tronconi, E. *J. Catal.* **2001**, *204*, 175.
(33) Nishino, T.; Sakurai, T.; Ishizawa, N.; Mizutani, N.; Kato, M. *J. Solid State Chem.* **1987**, *69*, 24.
(34) Strobel, R.; Maciejewski, M.; Pratsinis, S. E.; Baiker, A. *Thermochim. Acta* **2006**, in press.
(35) Karthikeyan, J.; Berndt, C. C.; Tikkanen, J.; Wang, J. Y.; King, A. H.; Herman, H. *Nanostruct. Mater.* **1997**, *8*, 61.
(36) Camenzind, A.; Strobel, R.; Pratsinis, S. E. *Chem. Phys. Lett.* **2005**, *416*, 193.

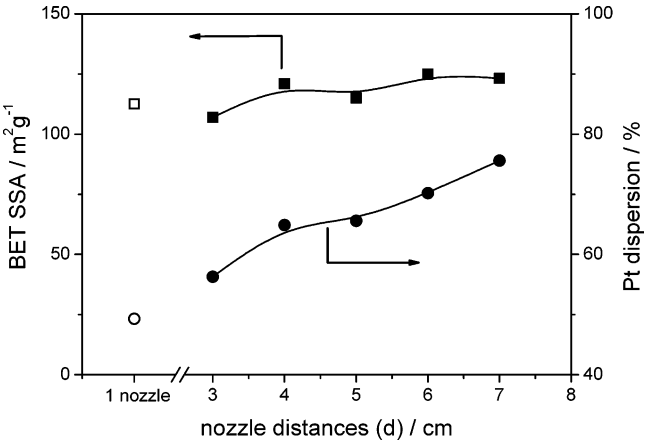

Figure 7. Platinum dispersion and SSA of $Pt/Ba/Al_2O_3$ made by FSP with either one or two nozzles as a function of internozzle distance (d).

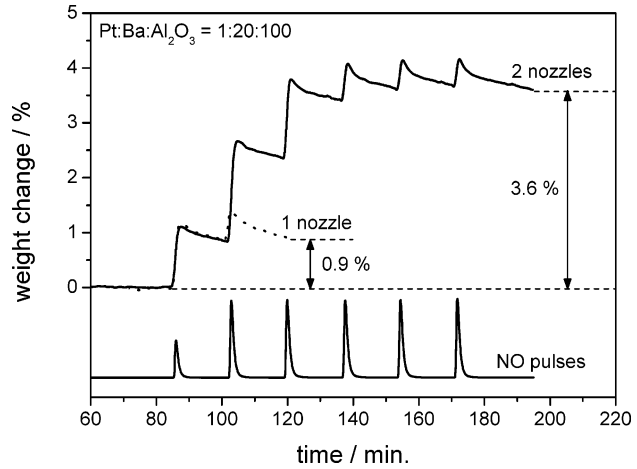

Figure 8. NO_x storage behavior of flame-derived $Pt/Ba/Al_2O_3$ made with one and two nozzles ($d = 6$ cm) as measured gravimetrically by injecting pulses of NO into 5 vol % O_2/He. MS trace ($m/z = 30$) indicating NO pulses in the outlet gas is shown at the bottom.

system. The amount of $BaCO_3$ increased with the internozzle distance up to 5 cm and leveled off close to the theoretical maximum.

Figure 7 shows the Pt dispersion and the SSA for $Pt/Ba/Al_2O_3$ prepared with either one nozzle or two nozzles as a function of the internozzle distance (d). The SSA of the product particles was hardly affected by the different nozzle geometries and the surface area increased only slightly with larger internozzle distances, indicating a small effect of the second flame on the Al_2O_3 particle formation process. In contrast, increasing the internozzle distance (d), the Pt dispersion increased from 56% ($d = 3$ cm) up to 75% ($d = 7$ cm). This is attributed to shorter Pt residence times at high temperatures as the later mixing of the two flames reduces the temperature encountered by Pt. As Pt particles form later at lower process temperatures compared to the Al_2O_3 particles,[9] the Pt dispersion is more affected by the additional heat contribution of the second flame at lower internozzle distance.

The influence of the previously discussed structural differences of one- or two-nozzle-made $Pt/Ba/Al_2O_3$ on the NO_x storage behavior is shown in Figure 8. The NO_x uptake was monitored gravimetrically and results in a mass increase of the catalysts by the formation of $Ba(NO_3)_2$ according to $BaCO_3 + 2\ NO_2 \rightarrow Ba(NO_3)_2 + CO_2$. A high mass increase

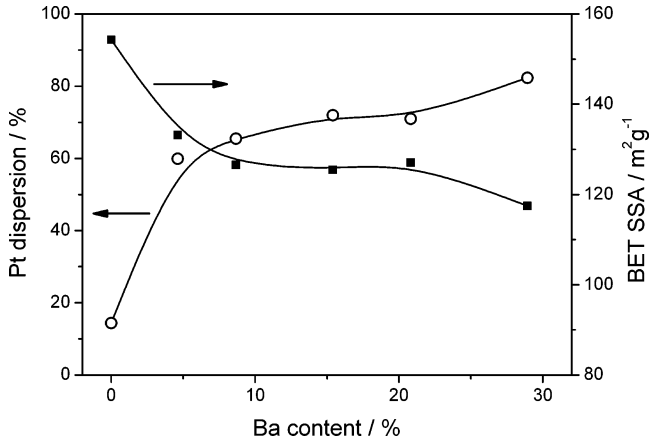

Figure 9. BET SSA and platinum dispersion as a function of the Ba content of $Pt/Ba/Al_2O_3$ made with two-nozzle FSP ($d = 6$ cm).

and thus a significant storage of NO_x in the form of $Ba(NO_3)_2$ was observed for $Pt/Ba/Al_2O_3$ made with two nozzles (3.6 wt %). In contrast, the powder made with one nozzle exhibited a very low mass uptake coming mainly from the adsorption of NO_x on the alumina surface. Therefore, it is evident that the formation of individual $BaCO_3$ particles as achieved by the two-nozzle process is crucial for the ability of the catalyst to store NO_x in the form of $Ba(NO_3)_2$. This is in agreement with the observations for conventionally prepared catalyst, where the formation of $BaAl_2O_4$ at high temperatures leads to the loss of NO_x storage capacity.[37,38] A thorough investigation of the NO_x storage and reduction behavior of flame-made $Pt/Ba/Al_2O_3$ concerning the influence of Ba content and nozzle setup in comparison with impregnated catalysts will be presented in a forthcoming study.

The influence of Ba content on the structural properties was investigated with powders consisting of $Pt/Ba/Al_2O_3 = 1{:}x{:}100$ with x ranging from 0 up to 50. Figure 9 shows the SSA and the Pt dispersion as a function of the Ba content (two nozzles at $d = 6$ cm). Compared to pure Pt/Al_2O_3, the addition of a small amount of Ba (4.6 wt % Ba) reduced the SSA from 155 to 133 m^2/g. However, adding more Ba had hardly any influence on the SSA. This is in contrast to impregnated Ba/Al_2O_3 catalysts, where the addition of Ba results in a high loss in SSA by clogging the pores of the support.[39] Flame-made materials are usually nonporous, and the high surface area comes only from the external surface of the nanoparticles.[7] For $Pt/Ba/Al_2O_3$ made with two spray nozzles, mainly Al_2O_3 contributes to the surface area. As the Al_2O_3 and $BaCO_3$ particles are formed separately no clogging occurs and the high surface area is retained.

The Pt dispersion increased with higher Ba contents (Figure 9). A large difference in Pt particle size was observed when changing the Ba content from 0 to 4.6 wt %. The Pt dispersion of no Ba containing Pt/Al_2O_3 made with two nozzles was much lower than that of Pt/Al_2O_3 made with one nozzle and similar Pt content as reported earlier.[7] For

(37) Elbouazzaoui, S.; Corbos, E. C.; Courtois, X.; Marecot, P.; Duprez, D. *Appl. Catal., B* **2005**, *61*, 260.
(38) Jang, B. H.; Yeon, T. H.; Han, H. S.; Park, Y. K.; Yie, J. E. *Catal. Lett.* **2001**, *77*, 21.
(39) Castoldi, L.; Nova, I.; Lietti, L.; Forzatti, P. *Catal. Today* **2004**, *96*, 43.

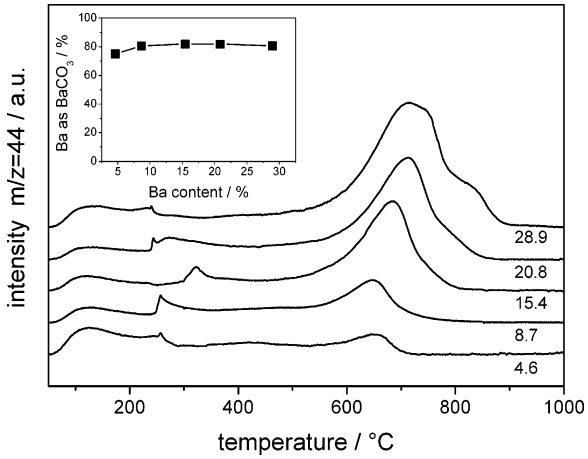

Figure 10. TPD CO_2 evolution profiles from $BaCO_3$ of flame-made Pt/Ba/Al_2O_3 with different Ba loadings (d = 6 cm). TPD was measured 1 month after sample preparation (Ba content (%) is shown on the curves). The inset depicts the amount of Ba in the form of $BaCO_3$ as derived from integrating the TPD profiles above 400 °C.

the Pt/Al_2O_3 powder made with two nozzles, Pt particles were formed separately in one flame without any Ba particles present. Noble metals tend to form larger particles (>20 nm) in the absence of a support.[40] If no Ba particles are present in the Pt containing flame, the Pt particle growth is not stopped until coagulation with Al_2O_3 particles from the other flame, and so larger Pt particles are observed. In contrast, in Ba containing powders the Pt particle growth is arrested on the $BaCO_3$ particles. For comparison a Pt/$BaCO_3$ powder was prepared containing no Al_2O_3 (Pt/Ba = 1:20). The Pt dispersion of this material was slightly lower (57%) than of a comparable Pt/Ba/Al_2O_3 made with two nozzles (i.e., 70% for d = 6 cm). This indicates that a small fraction of Pt is formed on the Al_2O_3 particles. It can be expected that co-formation of $BaCO_3$ and Pt in one flame ensures a close proximity of the Pt and $BaCO_3$ particles in the final product. This close contact between the two active species may be beneficial for NO_x storage reduction.[37]

Figure 10 depicts CO_2 evolution profiles from Pt/Ba/Al_2O_3 made at d = 6 cm containing different amounts of Ba. The experiments were carried out after complete transformation of monoclinic $BaCO_3$ into witherite, approximately 1 month after preparation. With higher Ba loadings the amount of CO_2, which evolved from $BaCO_3$ decomposition, increased. The relative amount of Ba in the form of $BaCO_3$ was always around 80% independent of Ba loading. Interestingly, not even for powders containing up to 28.9 wt % Ba the formation of so-called bulk or HT-$BaCO_3$ was observed. All materials made with the two-nozzle FSP process showed mainly formation of LT-$BaCO_3$. This behavior differs from that of Pt/Ba/Al_2O_3 catalysts prepared by impregnation, where no $BaCO_3$ was observed for low Ba contents and HT-$BaCO_3$ was the main form of Ba for high Ba loadings.[22] This makes the Pt/Ba/Al_2O_3 prepared with the two-nozzle FSP process a promising catalytic material for NSR.

Conclusions

A novel two-nozzle FSP process was developed for one-step synthesis of Pt/Ba/Al_2O_3 consisting of individually crystalline $BaCO_3$ and Al_2O_3 nanoparticles well-mixed at the nano-level. In contrast, amorphous Ba species dispersed over the Al_2O_3 particles were formed by the conventional single-nozzle FSP process. The formation of individual $BaCO_3$ particles as achieved by the two-nozzle process was beneficial for the NO_x storage behavior, whereas no NO_x was stored on the single-nozzle-made material. The amount of crystalline $BaCO_3$ could be controlled by varying the internozzle distance or in other words the point of mixing of the two flames. Increasing the Ba content did not clog the pores of the support as observed during wet impregnation and resulted only in a slight loss in SSA. Independent of the Ba loading the $BaCO_3$ nanoparticles decomposed at low temperatures (LT-$BaCO_3$) compared to bulk $BaCO_3$. This makes two-nozzle flame-made Pt/Ba/Al_2O_3 a promising material as a NSR catalyst.

Acknowledgment. The authors thank Dr. Frank Krumeich (ETH) for the TEM and ESI measurements. Financial support by the Swiss Commission for Technology and Innovation (KTI, Top Nano 21) and the Swiss Federal Institute of Technology (ETH, TH 2/03-2) is kindly acknowledged.

CM0600529

(40) Backman, U.; Tapper, U.; Jokiniemi, J. K. *Synth. Met.* **2004**, *142*, 169.